J|A|C|S
ARTICLES
Published on Web 03/01/2002

Switching "On" and "Off" the Expression of Chirality in Peptide Rotaxanes

Masumi Asakawa,[†] Giuseppe Brancato,[‡] Marianna Fanti,[‡] David A. Leigh,*[,||,⊥,▽] Toshimi Shimizu,[†] Alexandra M. Z. Slawin,[#] Jenny K. Y. Wong,[||,▽] Francesco Zerbetto,*[,‡,§] and Songwei Zhang[||]

Contribution from the Nanoarchitectonics Research Center, National Institute of Advanced Industrial Science and Technology, Tsukuba Central 5, 1-1-1 Higashi, Tsukuba, Ibaraki 305-8565, Japan, Dipartimento di Chimica "G. Ciamician", Università degli Studi di Bologna, V. F. Selmi 2, 40126, Bologna, Italy, Centre for Supramolecular and Macromolecular Chemistry, Department of Chemistry, University of Warwick, Coventry CV4 7AL, U.K., and School of Chemistry, University of St Andrews, North Haugh, St. Andrews, Fife KY16 9ST, U.K.

Received April 11, 2001. Revised Manuscript Received December 15, 2001

Abstract: The hydrogen-bond-directed synthesis, X-ray crystal structures, and optical properties of the first chiral peptide rotaxanes are reported. Collectively these systems provide the first examples of single molecular species where the expression of chirality in the form of a circular dichroism (CD) response can selectively be switched "on" or "off", and its magnitude altered, through controlling the interactions between mechanically interlocked submolecular components. The switching is achievable both thermally and through changes in the nature of the environment. Peptido[2]rotaxanes consisting of an intrinsically achiral benzylic amide macrocycle locked onto various chiral dipeptide (Gly-L-Ala, Gly-L-Leu, Gly-L-Met, Gly-L-Phe, and Gly-L-Pro) threads exhibit strong (10−20k deg cm^2 dmol^{-1}) negative induced CD (θ) values in nonpolar solvents (e.g. $CHCl_3$), where the intramolecular hydrogen bonding between thread and macrocycle is maximized. In polar solvents (e.g., MeOH), where the intercomponent hydrogen bonding is weakened, or switched off completely, the elliptical polarization falls close to zero in some cases and can even be switched to large positive values in others. Importantly, the mechanism of generating the switchable CD response in the chiral peptide rotaxanes is also determined: a combination of semiempirical calculations and geometrical modeling using the continuous chirality measure (CCM) shows that the chirality is transmitted from the amino acid asymmetric center on the thread via the macrocycle to the C-terminal stopper of the rotaxane. This understanding could have important implications for other areas where chiral transmission from one chemical entity to another underpins a physical or chemical response, such as the seeding of supertwisted nematic liquid crystalline phases or asymmetric synthesis.

Introduction

The absence of certain symmetry elements is the de facto requirement for chirality. Structures that possess only axes of symmetry or no symmetry at all—in fact the great majority of molecular shapes—are chiral, whereas those with a plane of symmetry (i.e., S_1), inversion center (S_2), or higher axes of rotoreflection (S_{3+}), are not. However, molecular level flexibility often permits the interconversion of low-symmetry enantiomeric shapes on short time scales such that many molecules are never effectively chiral despite principally adopting chiral conformations. While the presence of chirality is easily identifiable for any particular molecular structure, the *expression* of that chirality—i.e., the magnitude of the effects that the asymmetry has on the chemical and physical properties of the system—is much more elusive to quantify, understand, and, ultimately, control.[1] Sometimes the influence of a chiral center can be negligible; for example, a single asymmetric carbon atom at one end of a long alkyl chain generally has little effect on the properties of a prochiral center at the other end. Alternatively, the effects of molecular asymmetry can be greatly amplified; some chiral seed molecules need only be present in tiny amounts in order to induce and sustain the supertwist nematic phases exploited in liquid crystal displays. Control over the magnitude of the expression of chiral shape and associated phenomena is thus of great interest, particularly if it produces effects that can be triggered—or switched—through external stimuli.

Rotaxanes,[2] molecules consisting of a macrocyclic ring locked onto a linear "thread" by bulky "stoppers", are a class of compounds well-suited for exploring switchable phenomena.

* To whom correspondence should be addressed.
[†] Nanoarchitectonics Research Center.
[‡] Dipartimento di Chimica "G. Ciamician".
[||] Centre for Supramolecular and Macromolecular Chemistry.
[⊥] E-mail: David.Leigh@ed.ac.uk.
[▽] Current address: Department of Chemistry, University of Edinburgh, The King's Buildings, West Mains Road, Edinburgh EH9 3JJ, U.K.
[#] School of Chemistry.
[§] E-mail: gatto@ciam.unibo.it.

(1) For a recent comprehensive review on chiroptic molecular switches, see: Feringa, B. L.; van Delden, R. A.; Koumura, N.; Geertsema, E. M. *Chem. Rev.* **2000**, *100*, 1789−1816.

Several systems have been developed where the position of the macrocyclic ring can be switched from site to another—so-called "molecular shuttles"—in response to a range of stimuli, including light, electrons, pH, and the nature of the environment.[3] One of the major issues still to be properly explored with such architectures, however, is the nature of the physical and chemical effects that can be influenced utilizing mechanical bonding. Here we describe how a chiral optical response, circular dichroism, for hydrogen bond-assembled peptide rotaxanes[3d,4] with the general structure GlyX, where X is a chiral amino acid, can be controlled in terms of both magnitude and sign through the use of external stimuli which affect the intercomponent interactions between macrocycle and thread. The phenomenon is closely related to the ability of chiral species to induce an asymmetric response in the optical absorption bands of achiral partners (induced circular dichroism, ICD) through host−guest complexation[5] and represents the first examples of single molecular species where ICD can be selectively switched "on" or "off" through controlling the interactions between mechanically interlocked submolecular components. As a direct consequence of the tight fitting interlocked molecular architecture, switchable chiral transmission in peptide rotaxanes can be expressed over remarkably long distances.

Synthesis

The hydrogen bond-mediated synthesis of benzylic amide macrocycle-containing rotaxanes derived from achiral glycyl- and sarcosyl-(*N*-methyl glycine) dipeptide threads has previously been described.[3d,4a,b] Our mechanistic understanding of the five-component assembly process suggested that the route should allow the synthesis of rotaxanes based on any short oligopeptide sequence containing at least one non-N-terminus glycine residue.[6] Since all the coded α-amino acids besides glycine (and many uncoded and unnatural ones) possess asymmetric carbon atoms, this provides access to a virtually limitless range of main chain chiral rotaxanes where an asymmetric center is locked in close proximity to an intrinsically achiral macrocycle. Accordingly, a series of dipeptide threads **1**−**5** (Gly-L-Ala (**1**), Gly-L-Leu (**2**), Gly-L-Met (**3**), Gly-L-Phe (**4**), and Gly-L-Pro (**5**)) were prepared and converted into the corresponding chiral peptido[2]rotaxanes (**6**−**10**) in yields of 32−45%, for **6**−**9**, and 6%, for **10** (Scheme 1). The poor yield of the proline derivative is probably due to several factors including (i) the greater steric crowding of the hydrogen bonding sites of the thread by this bulky amino acid and (ii) the tertiary amide group stabilizing conformations of the thread which are unfavorable for rotaxane formation.

UV−Vis Spectroscopy and Circular Dichroism Experiments

To investigate the effect of the mechanical interlocking on the chiral environments of these systems, UV−vis absorption spectra (Figure 1 and Table 1) and circular dichroism measurements (Figures 2−4 and Table 2) in the wavelength region of aromatic ring excitation (230−320 nm) were carried out on dilute (0.1 mM) solutions of each thread and rotaxane in $CHCl_3$, MeCN, and MeOH. The solvents were chosen as being (i) relatively nonpolar ($CHCl_3$; the rotaxanes were insufficiently soluble in less polar solvents such as cyclohexane), (ii) polar, but uncompetitive for disrupting amide−amide hydrogen bonds (MeCN), and (iii) polar and competitive at solvent concentrations for disrupting amide-amide hydrogen bonds (MeOH; dimethyl sulfoxide, which we have previously used for breaking hydrogen bonds in amide rotaxane systems,[3d,4a,b] absorbs strongly in the UV−vis region of interest for this study). Note that the strong absorbance of all three solvents below 250 nm precludes accurate UV−vis measurements below this wavelength (which would have been desirable given that the trough of most of the CD responses of the peptide rotaxanes are in this region). The modest solubilities of the rotaxanes meant that higher concentrations of the substrates could not be used and, therefore, there may be a higher than usual error limit (∼10%) in the quantitative values of these experiments. Fortunately, however, the use of a 0.1 cm path length permitted the reproducible measurement of CD spectra in the range 230−

(2) (a) Schill, G. *Catenanes, Rotaxanes and Knots*, Academic Press: New York, 1971. (b) Chambron, J.-C.; Dietrich-Buchecker, C. O.; Sauvage, J.-P. *Top. Curr. Chem.* **1993**, *165*, 131−162. (c) Gibson, H. W.; Bheda, M. C.; Engen, P. T. *Prog. Polym. Sci.* **1994**, *19*, 843−945. (d) Amabilino, D. B.; Stoddart, J. F. *Chem. Rev.* **1995**, *95*, 2725−2828. (e) Leigh, D. A.; Murphy, A. *Chem., Ind*. **1999**, 178−183. (f) Sauvage, J.-P., Dietrich-Buchecker, C., Eds. *Molecular Catenanes, Rotaxanes and Knots*; Wiley-VCH: Weiheim, 1999. For chiral rotaxanes, see: (g) Archut, A.; Müller, W. M.; Baumann, S.; Habel, M.; Vögtle, F. *Liebigs Ann*. **1997**, 495−499. (h) Ashton, P. R.; Everitt, S. R. L.; Gómez-López, M.; Jayamaran, N.; Stoddart, J. F. *Tetrahedron Lett.* **1997**, *38*, 5691−5694. (i) Yamamoto, C.; Okamoto, T.; Schmidt, T.; Jäger, R.; Vögtle, F. *J. Am. Chem. Soc*. **1997**, *119*, 10547−10548. (j) Schimdt, T.; Schmieder, R.; Müller, W. M.; Kiupel, B.; Vögtle, F. *Eur. J. Org. Chem*. **1998**, 2003−2007. (k) Ashton, P. R.; Bravo, J. A.; Raymo, F. M.; Stoddart, J. F.; White, A. J. P.; Williams, *Eur. J. Org. Chem.* **1999**, *899*, 9−908. (l) Schmieder, R.; Hübner, G.; Seel, C.; Vögtle, F. *Angew. Chem. Int. Ed*. **1999**, *38*, 3528−3530.

(3) For examples of molecular shuttles and other stimuli-responsive rotaxanes, see: (a) Bissell, R. A.; Córdova, E.; Kaifer, A. E.; Stoddart, J. F. *Nature* **1994**, *369*, 133−137. (b) Ashton, P. R.; Ballardini, R.; Balzani, V.; Boyd, S. E.; Credi, A.; Gandolfi, M. T.; Gómez-López, M.; Iqbal, S.; Philp, D.; Preece, J. A.; Prodi, L.; Ricketts, H. G.; Stoddart, J. F.; Tolley, M. S.; Venturi, M.; White, A. J. P.; Williams, D. J. *Chem. Eur. J*. **1997**, *3*, 152−170. (c) Anelli, P.-L.; Asakawa, M.; Ashton, P. R.; Bissell, R. A.; Clavier, G.; Górski, R.; Kaifer, A. E.; Langford, S. J.; Mattersteig, G.; Menzer, S.; Philp, D.; Slawin, A. M. Z.; Spencer, N.; Stoddart, J. F.; Tolley, M. S.; Williams, D. J. *Chem. Eur. J*. **1997**, *3*, 1113−1135. (d) Lane, A. S.; Leigh, D. A.; Murphy, A. *J. Am. Chem. Soc*. **1997**, *119*, 11092−11093. (e) Murakami, H.; Kawabuchi, A.; Kotoo, K.; Kunitake, M.; Nakashima, N. *J. Am. Chem. Soc*. **1997**, *119*, 7605−7606. (f) Gong, C.; Glass, T. E.; Gibson H. W. *Macromolecules* **1998**, *31*, 308−313. (g) Armaroli, N.; Balzani, V.; Collin, J. P.; Gaviña, P.; Sauvage, J.-P.; Ventura, B. *J. Am. Chem. Soc*. **1999**, *121*, 4397−4408. (h) Shigekawa, H.; Miyake, K.; Sumaoka, J.; Harada, A.; Komiyama, M. *J. Am. Chem. Soc.* **122**, 5411 2000. (i) Ballardini, R.; Balzani, V.; Dehaen, W.; Dell'Erba, A. E.; Raymo, F. M.; Stoddart, J. F.; Venturi, M. *Eur. J. Org. Chem.* **2000**, 591−602. (j) Consuelo Jiménez, M.; Dietrich-Buchecker, C.; Sauvage, J.-P. *Angew. Chem. Int. Ed.* **2000**, *39*, 3284−3287. (k) Kawaguchi, Y.; Harada, A. *Org. Lett.* **2000**, *2*, 1353. (l) Bermudez, V.; Capron, N.; Gase, T.; Gatti, F. G.; Kajzar, F.; Leigh, D. A.; Zerbetto, F.; Zhang, S. *Nature* **2000**, *406*, 608−611. (m) Ashton, P. R.; Ballardini, R.; Balzani, V.; Credi, A.; Dress, K. R.; Ishow, E.; Kleverlaan, C. J.; Kocian, O.; Preece, J. A.; Spencer, N.; Stoddart, J. F.; Venturi, M.; Wenger, S. *Chem. Eur. J*. **2000**, *6*, 3558−3574. (n) Brouwer, A. M.; Frochot, C.; Gatti, F. G.; Leigh, D. A.; Mottier, L.; Paolucci, F.; Roffia, S.; Wurpel, G. W. H. *Science* **2001**, *291*, 2124−2128.

(4) (a) Leigh, D. A.; Murphy, A.; Smart, J. P.; Slawin, A. M. Z. *Angew. Chem., Int. Ed. Engl*. **1997**, *36*, 728−731. (b) Clegg, W.; Gimenez-Saiz, C.; Leigh, D. A.; Murphy, A.; Slawin, A. M. Z.; Teat, S. J. *J. Am. Chem. Soc*. **1999**, *121*, 4124−4129. (c) Leigh, D. A.; Troisi, A.; Zerbetto, F. *Angew. Chem. Int. Ed.* **2000**, *39*, 350−353.

(5) For ICD in host−guest complexes, see, for example: (a) Kodaka, M. *J. Am. Chem. Soc.* **1993**, *115*, 3702−3705. (b) Forman, J. E.; Barrans, R. E.; Dougherty, D. A. *J. Am. Chem. Soc.* **1995**, *117*, 9213−9228. (c) Yashima, E.; Matsushima, T.; Okamoto, Y. *J. Am. Chem. Soc*. **1997**, *119*, 6345−6359. (d) Asakawa, M.; Ashton, P. R.; Hayes, W.; Janssen, H. M.; Meijer, E. W.; Menzer, S.; Pasini, D.; Stoddart, J. F.; White, A. J. P.; Williams, D. J. *J. Am. Chem. Soc*. **1998**, *120*, 920−931. (e) Meillon, J.-C.; Voyer, N.; Biron, E.; Sanschagrin, F.; Stoddart, J. F. *Angew. Chem. Int. Ed.* **2000**, *39*, 143−145. For the use of hydrogen bonding to assemble remarkable chiral supramolecular arrays, see, for example: (f) Suárez, M.; Branda, N.; Lehn, J.-M.; Decian, A.; Fischer, J. *Helv. Chim. Acta* **1998**, *81*, 1−13. (g) Prins, L. J.; Huskens, J.; de Jong, F.; Timmerman, P.; Reinhoudt, D. N. *Nature* **1999**, *398*, 498−502. (h) Hirschberg, J. H. K. K.; Brunsveld, L.; Ramzi, A.; Vekemans, J. A. J. M.; Sijbesma, R. P.; Meijer, E. W. *Nature* **2000**, *407*, 167−170. (i) Prins, L. J.; de Jong, F.; Timmerman, P.; Reinhoudt, D. N. *Nature* **2000**, *408*, 181−184.

(6) Certain amino acids require chemical protection of sensitive functionality in order to be incorporated into rotaxanes by this synthetic strategy.

Scheme 1 The Syntheses of Peptide Rotaxanes **6**−**10** and **12**

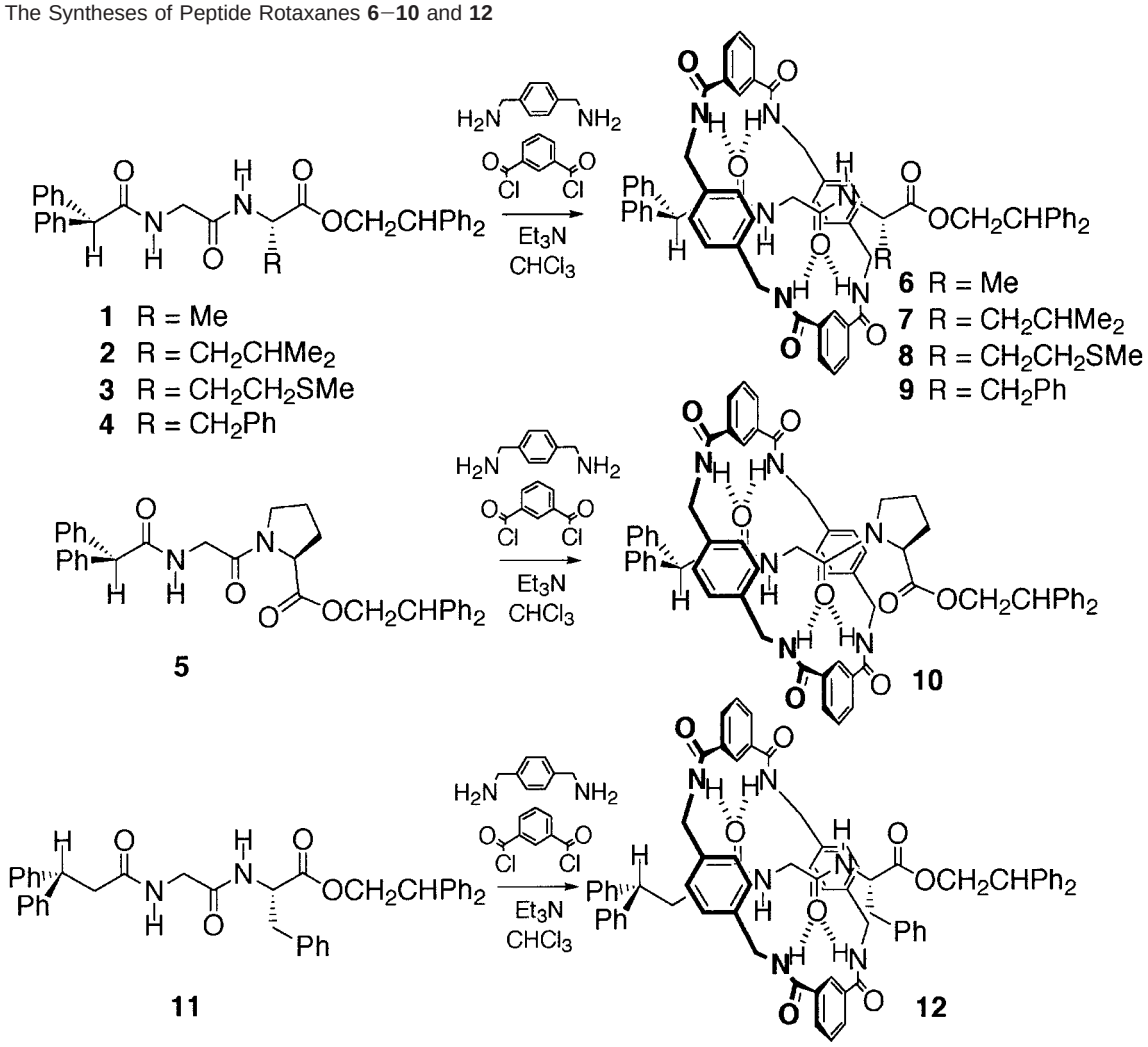

250 nm, even in $CHCl_3$, despite the strong absorbance of the solvent at these wavelengths. As a further control, identical CD measurements were also obtained using a different spectopolarimeter and experimental set up. *In all cases, the threads exhibited a zero CD response in each solvent system*, illustrating the lack of influence of the amino acid chiral centers on the four (five in the case of **4**) phenyl rings of the threads. In contrast, all five chiral peptide rotaxanes exhibited large molar ellipticities, the strength and sign of which varied with the nature of the solvent.

Figure 2 shows the room temperature CD spectra of the peptide rotaxanes in each solvent system. A number of general features are immediately apparent:

1. For each peptide rotaxane a strong negative ICD is observed in $CHCl_3$, the environment in which the intercomponent hydrogen bonding between macrocycle and thread is strongest. Since the CD response is absent in the spectra of each of the uninterlocked components, the ICD can be unambiguously attributed to the mechanically interlocked architecture of the system.

2. For each rotaxane in MeOH, the solvent in which the intercomponent hydrogen bonding is weakest, the magnitude of the ICD response is greatly reduced with respect to that in $CHCl_3$ and the *sign* of the response actually reversed in the case of the Gly-L-Ala, Gly-L-Met, and Gly-L-Phe rotaxanes **6**, **8**, and **9**.

3. The Gly-L-Leu and Gly-L-Phe rotaxanes (**7** and **9**) give comparable CD responses in MeCN and $CHCl_3$ suggesting that the co-conformations[7] adopted by the rotaxane components in these solvents are similar, the inference being that the intercomponent hydrogen bonding in these two rotaxanes is less easy to disrupt than in the other three systems.

4. For the various rotaxanes, the molar ellipticity in $CHCl_3$ varies between 5 and 20 000 deg cm^2 dmol^{-1} yet the active chromophore (be it on the stoppers or the macrocycle) is the same in each case! *Thus the size and shape of the amino acid substituent plays a crucial role in the efficient transmission of chiral information from the asymmetric center to the chromophore*.

The CD response of the Gly-L-Met rotaxane **8** is particularly noteworthy and Figures 3 and 4 show its dependence as a function of (a) the nature of the environment and (b) temperature. It has the largest magnitude room-temperature response of the dipeptide rotaxanes investigated here (−19900 deg cm^2 dmol^{-1} at a λ_{max} of 246 nm in $CHCl_3$) and the sign of the CD signal switches from negative to positive in MeOH (+3390 deg cm^2 dmol^{-1}) at a very similar wavelength (242 nm): a net change of >23000 deg cm^2 dmol^{-1} within a 4 nm range! The

(7) "Co-conformation" refers to the relative positions and orientations of the mechanically interlocked components with respect to each other [Fyfe, M. C. T.; Glink, P. T.; Menzer, S.; Stoddart, J. F.; White, A. J. P.; Williams, D. J. *Angew. Chem., Int. Ed. Engl.* **1997**, *36*, 2068−2069].

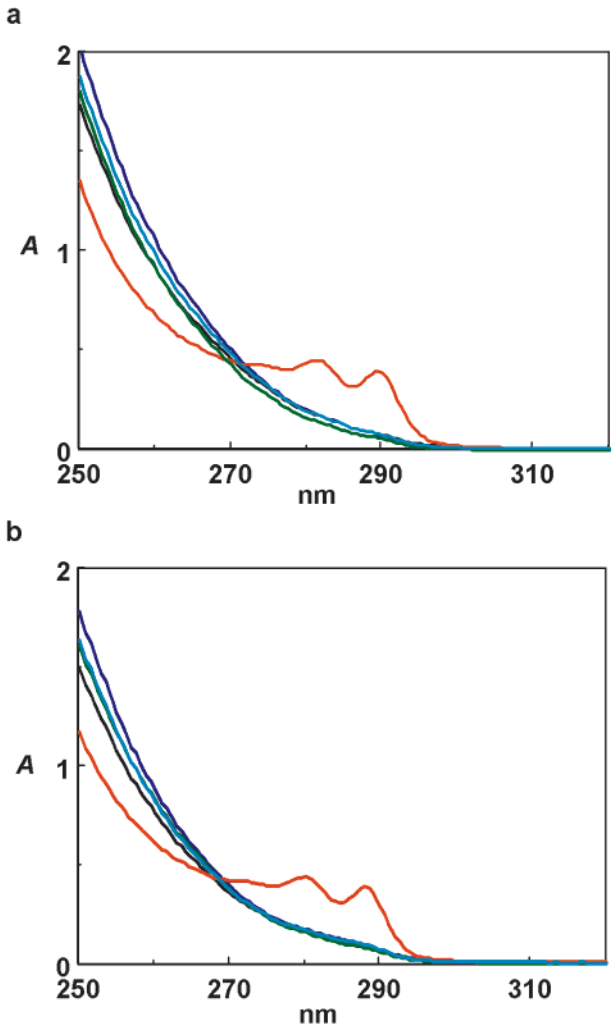

Figure 1. UV-visible spectra (0.1 mM) of peptide rotaxanes **6** (Gly-L-Ala, cyan), **7** (Gly-L-Leu, black), **8** (Gly-L-Met, blue), **9** (Gly-L-Phe, red), and **10** (Gly-L-Pro, green) in (a) MeOH, (b) $CHCl_3$. A = absorbance.

change in sign means that conditions exist (in this case 1:10 $CHCl_3$/MeOH at 298K, blue curve in Figure 3) where the chirality of **8** does *not* give rise to a CD response, but where it can be effectively switched "on"—to generate either a positive or negative value—by very small changes in the nature of the environment.

The sensitivity of the CD response that operates in these peptide rotaxanes and its dependence on the subtle nature of the intercomponent hydrogen bond strength between macrocycle and thread is well illustrated by the series of CD spectra shown in Figure 3. It is remarkable to note that adding an equal volume of MeOH to **8** in neat $CHCl_3$ (green and cyan curves, Figure 3) leads to only a 15% drop in signal intensity, yet going from 83% MeOH in $CHCl_3$ to neat MeOH (black and red curves, Figure 3), solutions of virtually identical polarity and dielectric constants, results in a switch in the CD response at 242 nm from -5590 to $+3390$ deg cm^2 dmol^{-1}!

The variation in the range of the CD response controllable by modulating the intercomponent hydrogen bonding by external factors is further demonstrated by the variable temperature CD spectra of **8** shown in Figure 4. In $CHCl_3$, where the intercomponent hydrogen bonding is strong, the CD response of **8** is unchanged over the range 263−333 K. However, in MeOH the signal is highly temperature dependent. At 263 K the CD response is large and *negative* suggesting that at low temperatures MeOH is unable to break the intercomponent hydrogen bonding, i.e., the co-conformation adopted by the rotaxane components is reminiscent of that adopted in $CHCl_3$. Increasing the temperature—i.e., increasing the ability of the solvent to disrupt the intercomponent hydrogen bonding—incrementally decreases the negative ICD signal, passing through zero, and ultimately leads to a large *positive* CD response at 333 K. The use of temperature to moderate both the size and handedness of the expression of a chiral response provides a further useful feature of these mechanically interlocked systems.

What Gives Rise to the ICD Signal?

The electronic (UV−vis) spectra of the rotaxanes in $CHCl_3$ and MeOH are shown in Figure 1. The spectra are largely structure and solvent invariant throughout the series, with absorption starting at wavelengths just below 300 nm (~35000 cm^{-1}) in agreement with that observed for other isophthalamide systems.[8] The electronically excited states of the phenyl groups of the macrocycle are conjugated with the π systems of the two adjacent carbonyl groups and have lower gaps than isolated phenyl rings. The lowest excited states of these systems are therefore a mixture of $n_o\pi^*$ and L_b (B_{2u} in D_{6h} symmetry) benzenic transitions. At about 250 nm (40000 cm^{-1}), the more intense benzenic L_a (B_{1u} in D_{6h} symmetry) states appear. The contribution of the macrocyclic ring to these transitions becomes evident if one compares the extinction coefficients of thread and rotaxane (Table 1). Significantly, the threads all have electronic transitions around 240−250 nm; in the corresponding rotaxanes, the states of the thread and macrocycle can be mixed through their degeneracy.

The molar ellipticities for the rotaxanes are given in Table 2 and the corresponding spectra shown in Figure 2. The main band is in the 240−250 nm region. In the hydrogen bond-disrupting solvent, MeOH, the bands are consistently smaller than in the non-hydrogen bond disrupting solvents, MeCN and $CHCl_3$. In MeOH the chiral peptide moiety can hydrogen bond to the solvent weakening or displacing the intramolecular hydrogen bonds that exist in a non-hydrogen bond disrupting solvent.

The ICD signal is clearly intrinsic to the mechanically interlocked molecular architecture of the peptide rotaxanes, since the resonances are absent for solutions of the uninterlocked, but otherwise chemically identical, components. While it is tempting to assume that the asymmetric center of the peptide simply forces the macrocycle chromophores (the aromatic rings) into a chiral environment giving rise to a CD response, this is not the only possible origin of the signal. The diphenylmethine stoppers also provide benzenic states which could elicit a CD response in the near UV, but like the aromatic rings of the macrocycle, they do not intrinsically carry any rotatory power and are too remote from the chiral center to be directly influenced by it (remember that none of the threads **1**−**5** exhibit a CD response in any of the solvents employed). Thus, the observed CD spectra must be caused by (long range) interactions between the chiral center and *either* the stoppers *or* the

(8) Brouwer, A. M.; Buma, W. J.; Caudano, R.; Fanti, M.; Fustin, C.-A.; Leigh, D. A.; Murphy, A.; Rudolf, P.; Zerbetto, F.; Zwier, J. M. *Chem. Phys.* **1998**, *238*, 421−428.

Table 1. Extinction Coefficients, ϵ, mol^{-1}, at Selected Wavelengths, Λ, nm, of Threads **1**−**5** and Rotaxanes **6**−**10** in $CHCl_3$

Threads					
nm	Gly-L-Ala (**1**)	Gly-L-Leu (**2**)	Gly-L-Met (**3**)	Gly-L-Phe (**4**)	Gly-L-Pro (**5**)
290	19	110	79	74	117
280	145	133	96	84	142
270	617	649	658	691	692
260	958	1020	1149	1198	1088
250	684	755	893	871	807
Rotaxanes					
nm	Gly-L-Ala (**6**)	Gly-L-Leu (**7**)	Gly-L-Met (**8**)	Gly-L-Phe (**9**)	Gly-L-Pro (**10**)
290	763	795	749	538	585
280	2088	1954	2004	1672	1621
270	4891	4610	5071	4307	4296
260	10133	9151	10553	9236	9165
250	18405	17413	20247	17148	18058

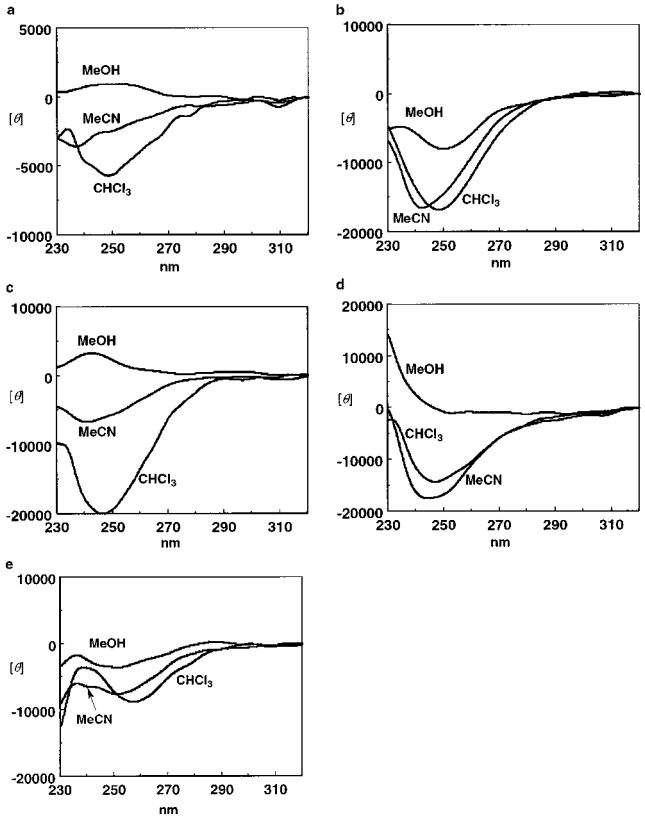

Figure 2. CD Spectra (0.1 mM) of (a) Gly-L-Ala rotaxane **6**, (b) Gly-L-Leu rotaxane **7**, (c) Gly-L-Met rotaxane **8**, (d) Gly-L-Phe rotaxane **9**, and (e) Gly-L-Pro rotaxane **10** in $CHCl_3$, MeCN, and MeOH at 298 K.

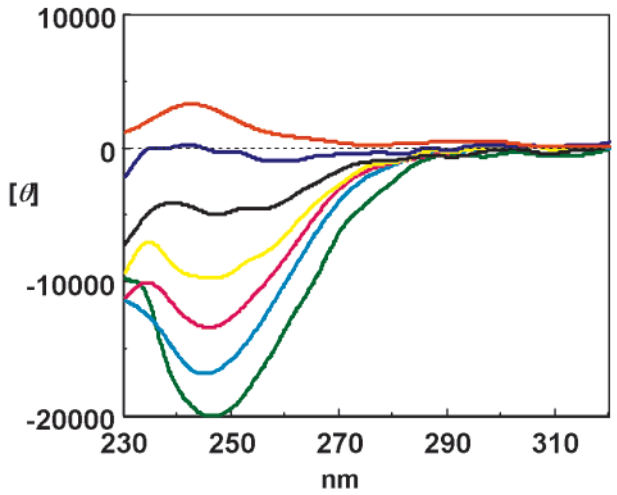

Figure 3. Environment-dependent CD spectra (0.1 mM) of Gly-L-Met rotaxane **8** in (a) 100% $CHCl_3$ (green), (b) 1:1 $CHCl_3$/MeOH (cyan), (c) 2:3 $CHCl_3$/MeOH (magenta), (d) 1:2 $CHCl_3$/MeOH (yellow), (e) 1:5 $CHCl_3$/MeOH (black), (f) 1:10 $CHCl_3$/MeOH (blue), and (g) 100% MeOH (red).

macrocycle aromatic chromophores, but it is not clear which. Evidence to distinguish between the two possibilities was provided by a combination of computer simulations and *X*-ray crystallography.

X-ray Crystallography

Four (**6**−**9**) of the five peptide rotaxanes studied provided single crystals suitable for structure determination by X-ray crystallography (Figure 5a−d). While care has to be taken when extrapolating from the solid-state to the situation in solution, these structures could be used to provide insights into the probable intercomponent interactions present and shape of the rotaxanes in nonpolar solvents. In particular, the crystal structures gave a starting point for understanding how the intercomponent hydrogen bonding interactions can effectively render either the macrocycle or stoppers chiral.

In principle, either the macrocycle or either of the N-terminus and C-terminus stoppers could be influenced by the chiral environment provided by the asymmetric center. When considered in isolation, the macrocycle in a boat conformation (close to that seen in the Gly-L-Ala crystal structure, Figure 5a) belongs to the C_{2v}, achiral, point group and in a chair conformation (close to that seen in the other three *X*-ray structures) to the achiral C_{2h} point group. Although rotation of a single amide group to point a carbonyl toward the cavity center effectively makes the macrocycle chiral (the faces of the ring are held in different environments, anyway: one points toward the N-terminus of the peptide, the other the C-terminus) there seems to be no reason for the macrocycle to do this and the absence of such conformations in any of the four crystal structures suggests against this possibility. The same considerations apply to the two phenyl groups of either stopper which could also assume chiral conformations but then would require suitable stabilization mechanisms to hold them in place. The large negative CD response is recorded for each of these four rotaxanes in $CHCl_3$, a situation where the conformations and co-conformations adopted by the rotaxane components is likely to be similar to those found in the solid-state X-ray crystal structures. The double

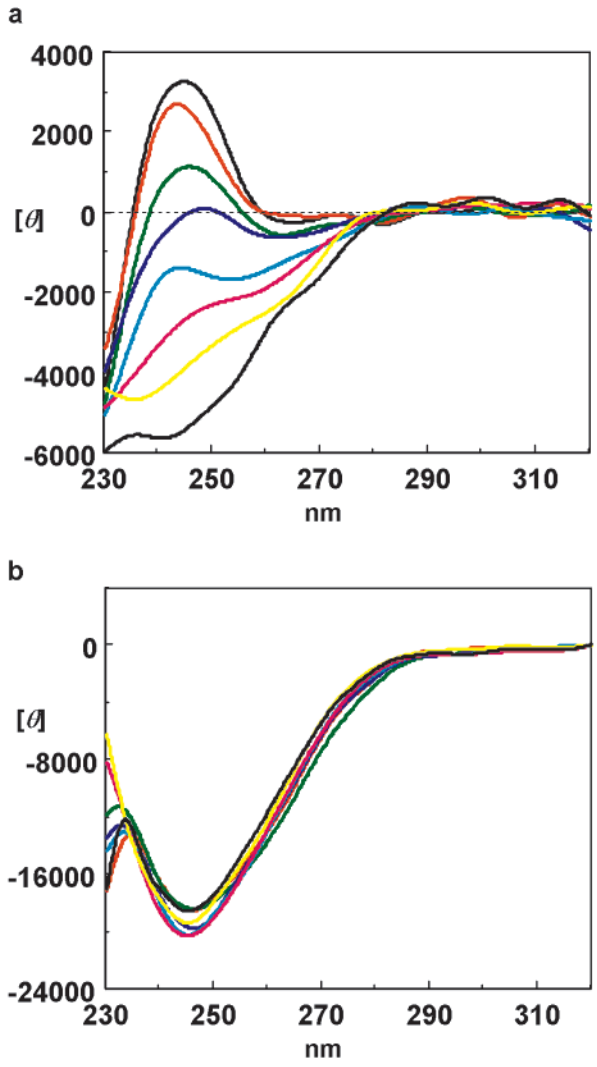

Figure 4. Temperature-dependent (263−333K) CD spectra (0.1 mM) of Gly-L-Met rotaxane **8** in (a) MeOH, (b) $CHCl_3$: 263 K (black), 273 K (red), 283 K (green), 293 K (blue), 303 K (cyan), 313 K (magenta), 323 K (yellow), and 333 K (black).

Table 2. Molar Ellipticities, θ, deg cm^2 dmol^{-1}, at Selected Wavelengths, λ, nm, of Chiral Peptide Rotaxanes **6**−**10**

rotaxane	solvent	λ	θ
Gly-L-Ala (**6**)	MeCN	237	−3530
	$CHCl_3$	248	−5670
	MeOH	252	+972
Gly-L-Leu (**7**)	MeCN	242	−16500
	$CHCl_3$	248	−16700
	MeOH	250	−7880
Gly-L-Met (**8**)	MeCN	241	−6580
	$CHCl_3$	246	−19900
	MeOH	242	+3390
Gly-L-Phe (**9**)	MeCN	242	−17300
	$CHCl_3$	247	−14500
	MeOH	251	−30
Gly-L-Pro (**10**)	MeCN	251	−7490
	$CHCl_3$	257	−8700
	MeOH	251	−3470

bifurcated hydrogen bond motif seen in each of the four X-ray structures effectively locks the macrocycle in place close to the chiral center. The stereochemistry of the amino acid dictates how one isophthaloyl unit of the macrocycle is situated below the hydrogen atom, rather than the more bulky alkyl substituent, of the chiral center. As well as providing a chiral environment for the macrocycle, this effectively locks the isophthaloyl ring extremely close to the C-terminus stopper whether the macrocycle adopts a boat (as with the Gly-L-Ala rotaxane, **6**) or a chair conformation (the other three cases).

The availability of the X-ray crystal structures of **6**−**9** also allowed us to undertake molecular modeling studies to pinpoint the origin of the CD signal using a combination of semiempirical calculations and geometrical modeling. The X-ray structures provide reliable geometries in all probability similar to those responsible for the ICD responses in $CHCl_3$.

Modeling the Spectroscopic Signatures

Modeling of the rotaxane CD spectra was performed with the intent of understanding the origin of the signal rather than quantitative analysis of the spectral patterns (see Experimental Section). First, the four rotaxanes (**6**−**9**) were considered in their entirety. For each rotaxane, the CD spectra were simulated[9] using the semiempirical procedure INDO/S (intermediate neglect of differential overlap/spectroscopic parametrization),[10] employing the *X*-ray crystal structures as starting geometries optimized with the MM3[11] model implemented in the TINKER[12] program. The approach is the same as that used previously to study the potential energy surface[13] and dynamics[14] of benzylic amide [2]catenanes in non-hydrogen-bonding solvents and their vibrations[15] in the solid state. Considering the size and the complexity of the system, the results are very satisfactory with the shape of the experimental curves accurately reproduced by the simulations (Figure 6). To understand which of the three sets of aromatic chromophores (C-terminus and N-terminus diphenylmethine stoppers and the macrocycle) were actually giving rise to the CD response, each was removed in turn (and replaced with hydrogen atoms in the case of the stoppers to maintain a chemically reasonable structure) and the spectra recalculated. Remarkably, when either the macrocycle or the N-terminus diphenylmethine stopper were removed from each rotaxane, the CD signal calculated was nearly the same as that found for the full system. However, in all cases the calculated CD response

(9) (a) Kaito, A.; Hatano, M. *Bull. Chem. Soc. Jpn.* **1980**, *53*, 3064−3068. (b) Oblink, J. H.; Hezemans, A. M. F. *Theor. Chim. Acta (Berlin)* **1976**, *43*, 75−87. (c) Michl, J. *Tetrahedron* **1984**, *40*, 3845−3934 and references therein; (d) West, R.; Downing, J. W.; Inagaki, S.; Michl, J. *J. Am. Chem. Soc.* **1981**, *103*, 5073−5078. (e) Orlandi, G.; Poggi, G.; Zerbetto, F. *Chem. Phys. Lett.* **1994**, *224*, 113−117. (f) Fanti, M.; Orlandi, G.; Poggi, G.; Zerbetto, F. *Chem. Phys.* **1997**, *223*, 159−168.
(10) (a) Del Bene, J.; Jaffé, H. H. *J. Chem. Phys.* **1968**, *48*, 1807−1813. (b) Nishimoto, K.; Mataga, N. *Z. Phys. Chem.* **1957**, *13*, 140−157. (c) Ellis R. L., Jaffé, H. H., Segal, G. A., Ed. In *Modern Theoretical Chemistry*; Plenum: New York, 1977; Vol. 4, p 49. (d) Pople, J. A.; Santry, D. P.; Segal, J. A. *J. Chem. Phys.* **1965**, *43*, S129−S135. (e) Ridley, J. E.; Zerner, M. C. *Theor. Chim. Acta* **1973**, *32*, 111−134. (f) Ridley, J. E.; Zerner, M. C. *Theor. Chim. Acta* **1976**, *42*, 223−236. (g) Zerner, M. C.; Loew, G. H.; Kirchner, R. F.; Mueller-Westerhoff, U. T. *J. Am. Chem. Soc.* **1980**, *102*, 589−599. (h) Edwards, W. D.; Zerner, M. C. *Theor. Chim. Acta* **1987**, *72*, 347−361. (i) Bendale, R. D.; Baker, J. D.; Zerner, M. C. *Int. J. Quantum Chem. Symp.* **1991**, *25*, 557−568.
(11) (a) Allinger, N. L.; Yuh, Y. H.; Lii, J.-H. *J. Am. Chem. Soc.* **1989**, *111*, 8551−8566. (b) Lii, J.-H.; Allinger, N. L.; *J. Am. Chem. Soc.* **1989**, *111*, 8566−8575. (c) Lii, J.-H.; Allinger, N. L.; *J. Am. Chem. Soc.* **1989**, *111*, 8576−8582.
(12) (a) Ponder, J.; Richards, F.; *J. Comput. Chem.* **1987**, *8*, 1016−1024. (b) Kundrot, C.; Ponder, J.; Richards, F. *J. Comput. Chem.* **1991**, *12*, 402−409. (c) Dudek, M. J.; Ponder, *J. Comput. Chem.* **1995**, *16*, 791−8169.
(13) Leigh, D. A.; Murphy, A.; Smart, J. P.; Deleuze M. S.; Zerbetto, F. *J. Am. Chem. Soc.* **1998**, *120*, 6458−6467.
(14) Deleuze M. S.; Leigh, D. A.; Zerbetto, F. *J. Am. Chem. Soc.* **1999**, *121*, 2364−2379.
(15) Caciuffo, R.; Degli Esposti, A.; Deleuze, M. S.; Leigh, D. A.; Murphy, A.; Paci, B.; Parker, S. F.; Zerbetto, F. *J. Chem. Phys.* **1998**, *109*, 11094−11100.

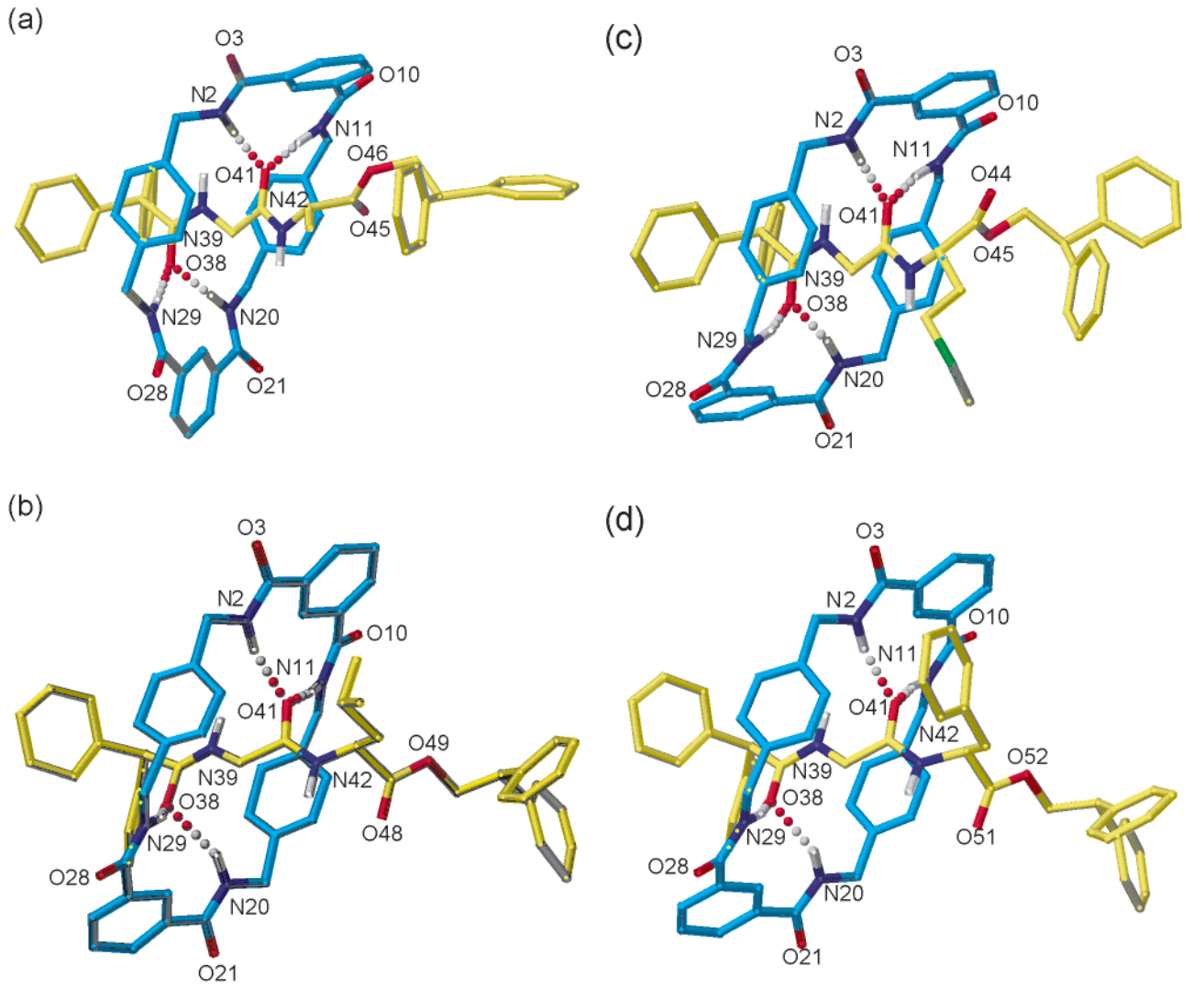

Figure 5. The solid-state structures of peptido[2]rotaxanes **6**−**9** as determined by X-ray crystallography. Carbon atoms of the macrocyclic ring are show in light blue and the carbon atoms of the peptide threads in yellow; oxygen atoms are depicted red, nitrogen atoms dark blue, and sulfur green. Nonamide hydrogen atoms have been removed for clarity; those indicated were placed in chemically reasonable positions: (a) Gly-L-Ala rotaxane **6**, intramolecular hydrogen bond distances (Å): O38−HN29 = 2.23, O38−HN20 = 1.89, O41−HN11 = 1.93, O41−HN2 = 1.95. Hydrogen bond angles (deg): O38−H−N29 = 174.1, O38−H−N20 = 162.7, O41−H−N11 = 170.9, O41−H−N2 = 167.5. (b) Gly-L-Leu rotaxane **7**, intramolecular hydrogen bond distances (Å): O38−HN29 = 1.97, O38−HN20 = 2.26, O41−HN11 = 1.98, O41−HN2 = 2.09. Hydrogen bond angles (deg): O38−H−N29 = 156.8, O38−H−N20 = 153.6, O41−H−N11 = 172.5, O41−H−N2 = 162.0. Selected dihedral angles (deg): C5−C4−C10−O10 = 158.0, C7−C8−C10−O10 = 158.7, C23−C22−C21−O21 = 155.4, C25−C26−C28−O28 = 140.2. (c) Gly-L-Met rotaxane **8**, intramolecular hydrogen bond distances (Å): O38−HN29 = 2.16, O38−HN20 = 1.87, O41−HN11 = 2.05, O41−HN2 = 1.90. Hydrogen bond angles (deg): O38−H−N29 = 157.5, O38−H−N20 = 162.3, O41−H−N11 = 165.4, O41−H−N2 = 171.7. Selected dihedral angles (deg): C5−C4−C3−O3 = 150.9, C7−C8−C10−O10 = 154.2, C25−C26−C28−O28 = 149.6, C23−C22−C21−O21 = 141.1. (d) Gly-L-Phe rotaxane **9**, intramolecular hydrogen bond distances (Å): O38−HN29 = 1.99, O38−HN20 = 2.18, O41−HN11 = 1.93, O41−HN2 = 2.13. Hydrogen bond angles (deg): O38−H−N29 = 160.3, O38−H−N20 = 149.4, O41−H−N11 = 169.3, O41−H−N2 = 164.8. Selected dihedral angles (deg): C7−C8−C10−O10 = 156.0, C5−C4−C3−O3 = 155.7, C25−C26−C28−O28 = 143.6, C23−C22−C21−O21 = 150.7.

was dramatically decreased by removal of the C-terminus diphenylmethine group. Details of the simulations are shown in Figure 6.

The Origin of the CD Response in Chiral Peptido[2]-rotaxanes

The nature of the well expressed chirality of the peptide rotaxanes in $CHCl_3$ can now be understood. The co-conformation seen in all the chiral peptide rotaxane X-ray crystal structures which places one of the isophthaloyl groups of the macrocycle under the hydrogen atom of the chiral center of the thread is locked in place in nonpolar solvents by the four intercomponent hydrogen bonds. In this position, the isophthaloyl group both restricts the rotation of the C-terminus diphenylmethine unit and destabilizes one or more of the three rotamers of the stopper, creating a well expressed chiral environment for the phenyl rings of the stopper which, in fact, are the chromophores responsible for the CD signal. Chiral information is thus transmitted from the asymmetric center on the thread to the macrocycle and on to the stopper of the thread. *Effectively, the tight fitting mechanically interlocked rotaxane architecture promotes a long distance chiral interaction.* Furthermore, with this mechanism of chiral transmission the ability of the different rotaxanes to modulate the magnitude of the CD signal can be attributed to the small angle variations

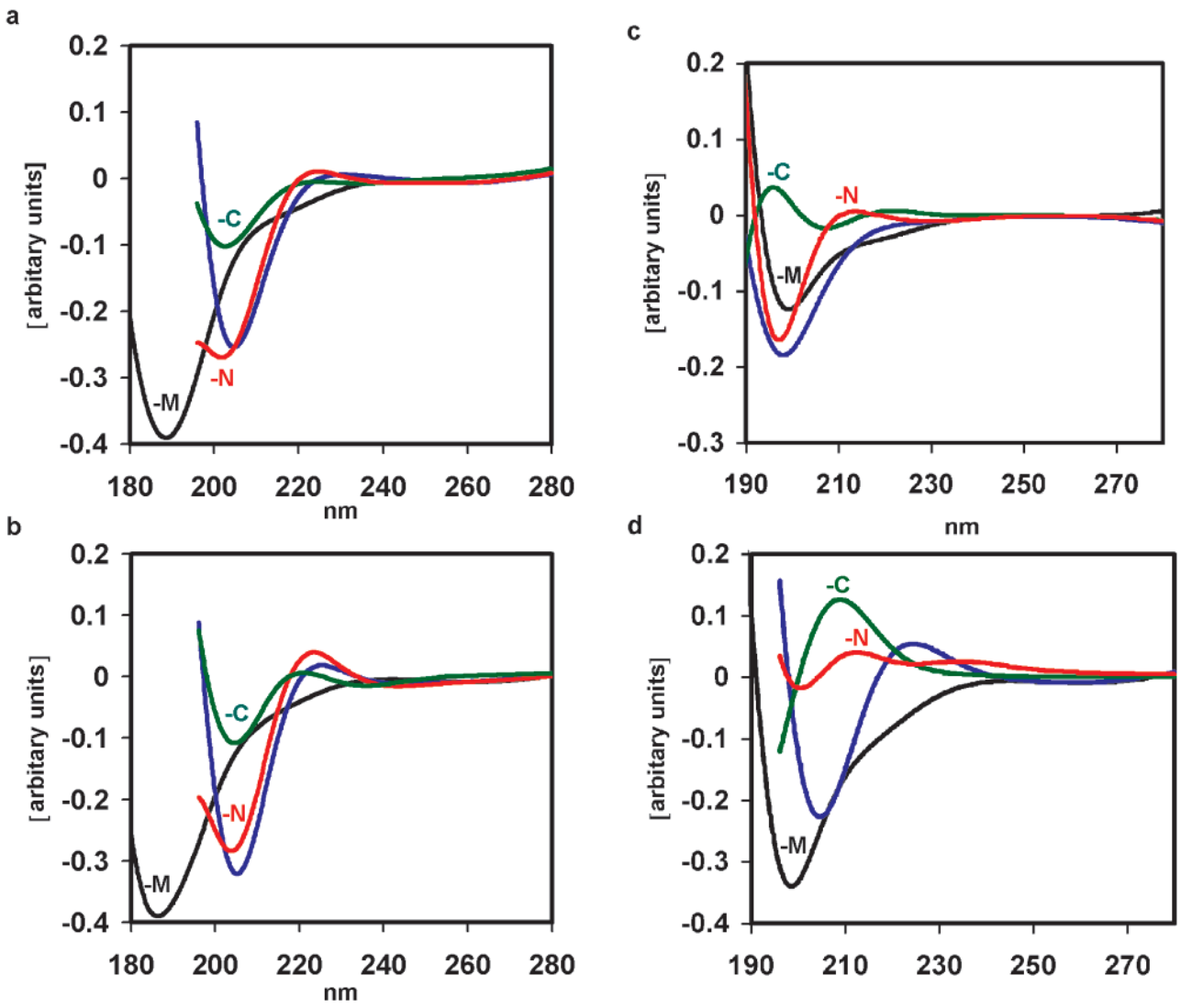

Figure 6. Simulated CD spectra of (a) Gly-L-Ala rotaxane **6**, (b) Gly-L-Leu rotaxane **7**, (c) Gly-L-Met rotaxane **8**, and (d) Gly-L-Phe rotaxane **9**, calculated as complete structures (blue curves, no label) and with each type of chromophore unit selectively removed: i.e., rotaxane-minus-N-terminus-stopper (red curves), rotaxane-minus-C-terminus-stopper (green curves), and rotaxane-minus-macrocycle (black curves).

that the two phenyl groups at the C-terminus can adopt in the different rotaxanes, a feature obviously determined by the size and shape of the alkyl substituents of the different amino acids in the rotaxanes.

It is also interesting to note that removal of the chromophore-bearing fragments shifts the spectral transitions to higher energy. In particular, removal of the macrocycle increases the energy of the main band by about 3000−5000 cm^{-1}, which, in turn, shows that, energetically, the ring takes part in the process although it does not, in the end, contribute to the CD signal itself. Its role is therefore to contribute to the electronic wave function and to the electric part of the transition dipole moment.

Testing the Hypothesis

To check that the C-terminus stopper is really the major contributor to the CD response of chiral peptide rotaxanes in nonpolar solvents, a further dipeptide rotaxane (**12**) was synthesized from a Gly-L-Phe thread (**11**) possessing a single additional methylene group between the ester unit and the C-terminus diphenylmethine stopper. This small structural change is well away from the hydrogen bonding motif used to template rotaxane formation (indeed, the yields of **9** and **12** are identical) and so should not affect the co-conformation adopted by the macrocycle and peptidic portion of the thread. However, the extra flexibility and small increase in distance provided by the extra methylene spacer should allow more facile rotation of the C-terminus diphenylmethine group and presumably place the phenyl rings in an environment where the chirality is less well expressed. Indeed, this is exactly what is found. The CD response of **12** in $CHCl_3$ is identical in shape and λ_{max} to that of **9**, but with an intensity reduced by 25% at all wavelengths. Similarly, replacing the C-terminus diphenylmethine stopper of **9** with a dicyclohexylmethine unit switches off the CD signal completely.

Quantifying the Expression of Chirality

While the modeling of the spectra with the removal of the chromophore-bearing fragments and their corroboration by experiment gives convincing results, the question arises as to whether one can quantify the amount of chirality the individual

Table 3. Continuous Chirality Measure of the Diphenylmethine Stoppers and the Macrocycle of Rotaxanes **6**−**9**

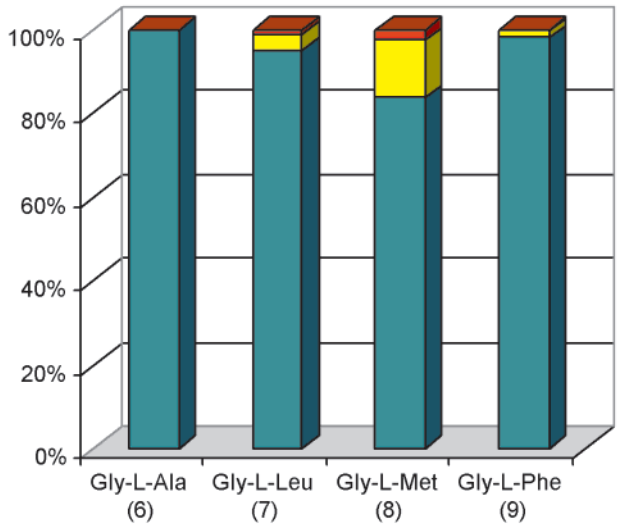

	Gly-L-Ala (**6**)	Gly-L-Leu (**7**)	Gly-L-Met (**8**)	Gly-L-Phe (**9**)
C-terminus stopper	1.122	1.569	0.031	1.659
macrocycle	0.001	0.064	0.005	0.032
N-terminus stopper	0.000	0.021	0.001	0.008

Table 4. Calculated Rotary Power of the First Four Transitions of Diphenylmethane for the Torsion of a Single Phenyl Group[a]

	0°[0.000]	15°[0.138]	30°[0.540]	45°[1.169]	60°[0.800]	75°[0.205]	90°[0.000]
S_1	0.00(270)	3.22(270)	5.08(270)	1.22(270)	−1.37(271)	−2.07(271)	0.00(271)
S_2	0.00(268)	−1.02(268)	−1.64(268)	1.63(268)	2.24(266)	1.53(265)	0.00(265)
S_3	0.00(234)	−18.30(233)	−30.20(230)	−31.89(227)	−25.01(222)	−15.94(218)	0.00(217)
S_4	0.00(209)	7.79(210)	16.20(211)	19.24(212)	12.64(213)	2.23(212)	0.00(209)

[a] In square brackets, the continuous chirality measure. (Notice that the torsion of a phenyl group changes the atoms that are reflected through the plane of symmetry.) In round brackets, the calculated excitation wavelength.

fragments contain and whether it relates to the calculated spectra. Quantitative techniques to measure the chirality have been proposed before. Here the continuous chirality measure,[16] CCM, was selected because it makes no assumption on a reference structure. CCM has already been found to rationalize a number of phenomena including the binding activities of trypsin/arylammonium inhibitors, D_2-dopamine receptor/dopamine derivative agonists, trypsin/organophosphates inhibitors, acetylcholinesterase/organophosphate and butyrylcholinesterase/organophosphates, carbon rearrangements in fullerenes, and the classification of enantiomerization pathways.[17] In the present context, the intent is to estimate the amount of chirality in the three chromophore-bearing fragments of the rotaxanes. Table 3 shows the chirality measures of the two stoppers and the macrocycle for each of the four peptide rotaxanes, **6**−**9**. In keeping with it being the major contributor to the CD response, the C-terminus diphenylmethine group has the largest chirality measure in all the rotaxanes, followed by the macrocycle. The N-terminus stopper is practically achiral in all cases, despite the X-ray structures suggesting that it is in more intimate contact with the macrocycle than the C-terminus unit. The simulation of the CD spectrum and the calculation of the CCM for a simple model system containing two phenyl groups supports the same conclusion. In Table 4, the rotatory power and the CCM are given for the torsion about a C−C bond of a phenyl group of diphenylmethane. Relatively small CCM suffice to give a large CD rotatory power similar to that seen for the Gly-L-Met rotaxane, **8**. The implication is that the CD spectrum is a highly nonlinear function of CCM.

Conclusions

The mechanically interlocked architectures of readily accessible, main-chain chiral peptido[2]rotaxanes enable them to exhibit a remarkable form of physical behavior, namely the variation in *size* and, in some cases, even the *sign* of their chiral response (observed through circular dichroism) as a result of changes in the nature of their local environment or thermal stimuli. In the absence of strong intercomponent interactions (e.g., in polar solvents at ambient and higher temperatures), the macrocycle is able to move relatively freely with respect to the thread and the chiral center is not effective in inducing a chiral environment for chromophores present on the macrocycle or stoppers. Under appropriate conditions (e.g., at low temperatures or in nonpolar solvents), however, when the intercomponent interactions are strong and highly directional, the steric requirements of the chiral center at the periphery of the hydrogen bonding template forces the macrocycle to adopt a very specific coconformation with the thread. Consequently, the conforma-

(16) (a) Zabrodsky, H.; Avnir, D. *J. Am. Chem. Soc.* **1995**, *117*, 462−473. (b) Avnir, D.; Katzenelson, O.; Helor, H. Z. *Chem. Eur. J.* **1996**, *2*, 744−746. (c) Katzenelson, O.; Helor, H. Z.; Avnir, D. *Chem Eur. J.* **1996**, *2*, 174−181.

(17) (a) Krinan, S.; Avnir, D. *J. Am. Chem. Soc.* **1998**, *120*, 6152−6159. (b) Pinto, Y.; Fowler, P. W.; Mitchell, D.; Avnir, D. *J. Phys. Chem. B* **1998**, *102*, 5776−5784. (c) Pinto, Y.; Salomon, Y.; Avnir, D. *J. Math. Chem.* **1998**, *23*, 13−29.

tionally fixed macrocycle locks the diphenylmethine group of the C-terminus stopper into a chiral environment, generating a CD response.

In light of the mechanism of CD signal generation, the success of the spectral simulations and the sizes of the CCM's, the expression of chirality is shown to be a nonlinear effect that can effectively be transmitted over long distances via bridges of low asymmetry. The generality and wide applicability of the CCM means that the induction of chirality into the C-terminus stopper may manifest itself beyond a simple ICD response. *Thus the switching "on" and "off" of the expression of chirality in peptide rotaxanes by controlling intercomponent interactions, i.e., through the "mechanical bond", may be a general phenomenon, not limited to a simple optical response*. This understanding could have important implications for other areas where chiral transmission from one chemical entity to another underpins a physical or chemical response, such as the seeding of supertwisted nematic liquid crystalline phases or asymmetric synthesis.

Experimental Procedures

General Method for the Preparation of Benzylic Amide Macrocycle-Containing Chiral Peptido[2]rotaxanes. The enantiopure[18] L-configuration amino acid dipeptide threads (**1**−**5**, **11**, 0.96 mmol) and triethylamine (1.55 g, 15.4 mmol) were dissolved in anhydrous chloroform (200 mL) and stirred vigorously, while solutions of xylylene diamine (7.68 mmol) in anhydrous chloroform (40 mL) and isophthaloyl chloride (7.68 mmol) in anhydrous chloroform (40 mL) were simultaneously added over a period of 4 h using motor-driven syringe pumps. The resulting suspension was filtered and concentrated under reduced pressure to afford the crude product which was then washed with ethyl acetate to leave only the unconsumed thread and [2]rotaxane in solution. This mixture was subjected to column chromatography (silica gel, CH_2Cl_2/MeOH as eluent) to yield, in order of elution, the unconsumed thread and the corresponding peptido[2]rotaxane (**6**−**10**, **12**). Selected data for [2]-(1,7,14,20-tetraaza-2,6,15,19-tetraoxo-3,5,9,12,16,18,22,25-tetrabenzocyclohexacosane)-(diphenylacetylglycylalaninate 2,2-diphenylethyl ester)-rotaxane (**6**): yield 45%; mp 238−239 °C; ^{1}H NMR (400 MHz, $CDCl_3$) δ 8.32 (s, 2H, isophthaloyl 2-*H*), 8.31 (d, 1H, CON*H*CH), 8.16 (d, 2H, J = 7.6 Hz, isophthaloyl 5-*H*), 8.14 (d, 2H, J = 7.6 Hz, isophthaloyl 4-*H* and 6-*H*), 7.58 (t, 4H, broad, macrocyclic N*H*CH_2), 7.3−7.0 (m, 20H, Ar*H*), 6.89, 6.79 (d, 8H, J = 7.7 Hz, *p*-xylylenediamine Ar-*H*), 5.60 (t, 1H, J = 3.5 Hz, CON*H*CH_2), 4.65 (d, 1H, J = 5.0 Hz, OC*H*H′CH), 4.61 (d, 1H, J = 5.0 Hz, OCH*H*′CH), 4.5−4.0 (m, 8H, macrocyclic NHCH_2), 4.31 (s, 1H, Ph_2C*H*CO), 4.10 (t, 1H, J = 5.0 Hz, CH_2C*H*Ph_2), 3.78 (m, 1H, NHC*H*CO), 2.64 (dd, 1H, J = 3.5 Hz, NHC*H*H′CO) 2.45 (dd, 1H, J = 3.5 Hz, NHCH*H*′CO), 0.98 (d, 3H, J = 4.6 Hz, CHCH_3); ^{13}C NMR (100 MHz, 10% CD_3OD in $CDCl_3$) δ 178.60, 172.45, 171.55, 166.78, 165.55, 140.50, 138.88, 137.68, 134.19, 131.95, 129.70, 129.46, 129.06, 128.99, 128.81, 128.75, 128.38, 128.32, 128.09, 127.43, 127.36, 124.56, 67.43, 58.18, 51.22, 48.81, 43.98, 41.80, 29.62, 16.33; FAB-MS (*m*NBA matrix) *m*/*z* 1053 [(rotaxane+H)$^+$]. Anal. Calcd for $C_{65}H_{60}N_6O_8$: C 74.1, H 5.7, N 8.0. Found: C 74.4, H 5.9, N 7.6. Selected data for [2]-(1,7,14,20-tetraaza-2,6,15,19-tetraoxo-3,5,9,12,16,18,22,25-tetrabenzocyclohexacosane)-(diphenylacetylglycylleucine 2,2-diphenylethyl ester)-rotaxane (**7**): yield 37%; mp 278−280 °C; ^{1}H NMR (400 MHz, $CDCl_3$) δ 8.18 (t, 4H, J = 7.7 Hz, isophthaloyl 4-H 6-H), 8.15 (s, 2H, isophthaloyl 2-H), 7.77 (d, 1H, broad, Leu N*H*CHCO), 7.62 (t, 2H, J = 7.7 Hz, isophthaloyl 5-H), 7.06−7.30 (m, 20H, thread Ar-*H*), 6.99 (d, 4H, AA′BB′ system, J = 8.0 Hz, *p*-xylylenediamine Ar-H_a), 6.90 (d, 4H, AA′BB′ system, J = 8.0 Hz, *p*-xylylenediamine Ar-H_b), 5.52 (t, 1H, J = 3.5 Hz, Gly CON*H*CHH′), 4.73 (m, 1H, Leu NHC*H*CO), 4.45 (m, 2H, COOCH_2-$CHPh_2$), 4.40 (m, 8H, macrocyclic CH_2NH), 4.26 (s, 1H, thread Ph_2C*H*CO), 3.96 (m, 1H, $COOCH_2$C*H*Ph_2), 2.75 (d, 2H, J = 3.6 Hz, Gly NHCH_2CO), 1.25 (m, 3H, CH_2C*H*$(CH_3)_2$ and CH_2CH$(CH_3)_2$); 0.72 (d, 3H, J = 6.0 Hz, $CH_2CHCH_3CH'_3$), 0.66 (d, 3H, J = 6.0 Hz, CH_2-$CHCH_3CH'_3$); ^{13}C NMR (100 MHz, $CDCl_3$) δ = 172.29, 172.12, 169.08, 167.15, 166.85, 140.31, 138.71, 137.12, 136.84, 133.81, 131.46, 129.24, 128.81, 128.69, 128.61, 128.31, 127.92, 127.82, 127.50, 126.91, 124.52, 67.30, 57.82, 51.19, 43.83, 40.30, 29.56, 24.36, 21.90; FAB-MS (*m*NBA matrix) *m*/*z* 1095 [(rotaxane+H)$^+$]. Anal. Calcd for $C_{68}H_{66}N_6O_8$: C 74.6, H 6.0, N 7.7. Found: C 75.0, H 6.2, N 7.5. Selected data for [2]-(1,7,14,20-tetraaza-2,6,15,19-tetraoxo-3,5,9,12,-16,18,22,25-tetrabenzocyclohexacosane)−(diphenylacetylglycylmethionine 2,2-diphenylethyl ester rotaxane (**8**): yield 36%; mp 261−262 °C; ^{1}H NMR (400 MHz, $CDCl_3$): δ 8.36 (s, 2H, isophthaloyl 2-H), 8.23 (d, 2H, J = 8.0 Hz, isophthaloyl 4-H), 8.18 (d, 2H, J = 8.0, isophthaloyl 6-H), 7.62 (t, 2H, J = 8.0 Hz, isophthaloyl 5-H), 7.47, (m, 4H, broad, macrocyclic N*H*), 7.07−7.23 (m, 20H, thread stoppers Ar-*H*), 6.92 (d, 4H, J = 7.8 Hz, *p*-xylylenediamine Ar-H_a), 6.84 (d, 4H, J = 7.8 Hz, *p*-xylylene Ar-H_b), 5.57 (m, 1H, broad, Gly CON*H*CH_2), 4.74 (m, 1H, Met NHC*H*CO), 4.48 (m, 3H, $COOCH_2$-$CHPh_2$ and COOCH2$CHPh_2$), 4.35 (m, 8H, macrocyclic $NHCH_2$), 4.26 (s, 1H, thread Ph_2CHCO), 2.62 (m, 2H, broad, Gly $NHCH_2CO$), 2.13 and 2.08 (m, 4H, Met $CHCH_2CH_2SCH_3$), 1.80 (s, 3H, Met $CHCH_2$-CH_2SCH_3); ^{13}C NMR (100 MHz, $CDCl_3$): δ 171.98, 171.29, 168.76, 167.34, 167.01, 140.18, 140.04, 138.91, 136.71, 136.69, 133.75, 130.70, 130.54, 128.68, 128.53, 128.26, 128.14, 127.62, 126.92, 126.60, 125.37, 67.81, 57.32, 50.86, 50.79, 43.81, 43.70, 30.10, 29.04, 14.00; FAB-MS (*m*NBA matrix) *m*/*z* 1113 [(rotaxane+H)$^+$]. Anal. Calcd. for $C_{67}H_{64}N_6O_8S$: C 72.3, H 5.7, N 7.5, S 2.9. Found: C 72.8, H 5.8, N 7.8, S 2.7. Selected data for [2]-(1,7,14,20-tetraaza-2,6,15,19-tetraoxo-3,5,9,12,16,18,22,25-tetrabenzocyclohexacosane)-(diphenylacetylglycylphenylalanine 2,2-diphenylethyl ester)-rotaxane (**9**): yield 32%; mp 227−229 °C; ^{1}H NMR (400 MHz, $CDCl_3$) δ 8.35 (s, 2H, isophthaloyl 2-*H*), 8.22 (t, 4H, J = 7.7 Hz, isophthaloyl 4-*H*, 6-*H*), 7.65 (t, 2H, J = 7.7 Hz, isophthaloyl 5-H), 7.39 (t, 4H, broad macrocyclic CON*H*CHH′), 7.08−7.26 (m, 25H, Ar-*H* of thread); 6.97 (d, 1H, J = 6.8 Hz, Phe N*H*CHCO), 6.74 (d, 4H, AA′BB′ system J = 7.8 Hz, *p*-xylylenediamine Ar-H_a), 6.50 (d, 4H, AA′BB′ system J = 7.8 Hz, *p*-xylylenediamine Ar-H_b), 5.38 (t, 1H, broad, Gly N*H*CH_2CO), 4.70 (m, 1H, Phe NHC*H*CO), 4.40 (m, 2H, COOCH_2CHPh$_2$), 4.24 (m, 1H, $COOCH_2$-C*H*Ph_2), 4.14 (s, 1H, Ph_2C*H*CO), 4.08 (m, 8H, macrocyclic CH_2NH), 2.58 (m, 2H, Gly CONHCH_2), 2.52 (m, 2H, Phe C*HH*′Ph); ^{13}C NMR (100 MHz, $CDCl_3$) δ 171.58, 170.78, 169.31, 167.58, 166.73, 139.74, 138.48, 136.57, 136.22, 133.57, 133.51, 130.85, 130.75, 128.79, 128.60, 128.54, 128.46, 128.35, 128.18, 128.02, 127.56, 127.49, 127.01, 126.37, 124.60, 67.40, 56.64, 50.34, 53.55, 49.87, 43.45, 43.03, 36.56; FAB-MS (*m*NBA matrix) *m*/*z* 1129 [(rotaxane+H)$^+$]. Anal. Calcd for $C_{71}H_{64}N_6O_8$: C 75.5, H 5.7, N 7.5. Found: C 74.5, H 5.5, N 7.3. Selected data for [2]-(1,7,14,20-tetraaza-2,6,15,19-tetraoxo-3,5,9,12,16,-18,22,25-tetrabenzocyclohexacosane)-(diphenylacetylglycylproline 2,2-diphenylethyl ester)-rotaxane (**10**): yield 6%; ^{1}H NMR (400 MHz, $CDCl_3$) δ 8.50 (s, 2H, isophthaloyl 2-H), 8.39 (d, 2H, J = 8.0 Hz, isophthaloyl 4-H or 6-H), 8.30 (d, 2H, J = 8.0 Hz, isophthaloyl 4-H or 6-H), 7.69 (t, 2H, J = 8.0 Hz, isophthaloyl 5-H), 7.6−6.9 (m, 20H, Ar-*H*), 6.94 (d, 4H, J = 8.0 Hz, xylylene-H_a), 6.78 (d, 4H, J = 8.0 Hz, xylylene-H_b), 5.66 (broad, 1H, CON*H*CH_2), 4.74 (dd, 1H, J = 15.0 Hz, 8 Hz, OC*H*H′CHPh$_2$), 4.60 (broad, 4H, macrocyclic NHC*H*H′), 4.40 (s, 1H, Ph_2CHCO), 4.30 (broad, 4H, macrocyclic NHCH*H*′), 4.08 (m, 1H, OCH*H*′CHPh$_2$), 3.82 (dd, 1H, J = 8.0 Hz, 5 Hz, OC*H*H′CH), 2.85 (d, 1H, J = 6.0 Hz, NHCH*H*′CO), 2.80 (m, 1H, Pro NC*H*H′CH_2), 2.60 (m, 1H, Pro NCH*H*′CH_2), 2.52 (d, 1H, J = 5.0 Hz, Gly NHCH*H*′CO), 2.45 (d, 1H, J = 5.0 Hz, Gly NHC*H*H′CO), 1.9−1.3 (m, 4H, Pro $NCH_2CH_2CH_2CH$); ^{13}C NMR (100 MHz, $CDCl_3$) δ 172.45, 171.01 167.80, 165.78, 141.55, 138.23, 137.56, 136.26, 133.75, 131.45, 129.34, 128.84, 128.28, 128.78 128.43, 127.42, 127.14, 127.00, 126.89,

(18) Racemic Gly-DL-Phe rotaxane (**4**) was prepared as a control and, as expected, did not give a CD response in any solvent.

124.52, 72.54, 68.37, 56.72, 52.10, 43.80, 41.39, 30.78, 25.56, 20.38 19.55; FAB-MS (*m*NBA matrix) *m*/*z* 1079 [(rotaxane+H)$^+$]. Anal. Calcd for $C_{67}H_{62}N_6O_8$: C 74.6, H 5.8, N 7.8. Found: C 74.0, H 5.9, N 7.7. Selected data for [2]-(1,7,14,20-tetraaza-2,6,15,19-tetraoxo-3,5,9,-12,16,18,22,25-tetrabenzocyclohexacosane)-(diphenylacetylglycylphenylalanine 3,3-diphenyl-1-propyl ester)-rotaxane (**12**): yield 42%; mp 260−262 °C; ^{1}H NMR (400 MHz, $CDCl_3$) δ 8.19 (t, 4H, J = 8.3 Hz, isophthaloyl 4-*H* and 6-*H*), 8.18 (s, 2H, isophthaloyl 5-*H*), 7.61 (t, 2H, J = 8.3 Hz, isophthaloyl 2-*H*), 7.37 (t, 2H, J = 5.3 Hz, macrocyclic N*H*), 7.36−7.10 (m, 25H, thread Ar-*H*), 7.04 (t, 2H, J = 5.4 Hz, macrocyclic N*H*), 6.89 (d, 4H, AA′BB′ system J = 8.0 Hz, *p*-xylylene Ar-H_a), 6.76 (d, 4H, AA′BB′ system J = 8.0 Hz, *p*-xylylene Ar-H_b), 5.47 (t, 1H, broad, Gly N*H*CH_2CO), 4.44 (dd, 4H, J = 4.5 Hz, 13.9 Hz, macrocyclic C*H*H′NH), 4.31 (dd, 4H, J = 4.5 Hz, 13.9 Hz, macrocyclic CH*H*′NH), 4.19 (s, 1H, Ph_2CHCO), 3.98 (m, 1H, $COOCH_2$-$CH_2CH$$Ph_2$), 3.82 (m, 2H, $COOCH_2CH_2CHPh_2$), 3.81 (m, 1H, Phe NHC*H*CO), 3.11 (dd, 1H, J = 5.0 Hz, 14.1 Hz, Phe C*H*H′Ph), 2.88 (dd, 1H, J = 9.5 Hz, 13.9 Hz, Phe CH*H*′Ph), 2.76 (m, 2H, broad, Gly CONHCH_2); 2.14 (m, 2H, $COOCH_2CH_2CHPh_2$); ^{13}C NMR (100 MHz, $CDCl_3$) δ 172.49, 171.23, 170.15, 166.89, 166.73, 143.94, 138.78, 138.70, 137.66, 137.22, 136.19, 134.27, 134.17, 132.15, 131.89, 129.71, 129.21, 129.15, 128.78, 128.28, 128.18, 128.07, 127.99, 126.94, 124.14, 64.89 (COO*C*HH′CHH′CHPh$_2$), 58.68 (Ph_2*C*HCO), 55.46 (Phe NH-C*H*CO), 48.05, (COOCHH′CHH′*C*HPh$_2$), 44.61, 44.44, (macrocyclic NH*C*H$_2$), 42.66 (Gly CONHC*H*H′), 37.93 (Phe CH*C*HH′Ph), 34.21 (COOCHH′*C*HH′CHPh$_2$); FAB-MS (*m*NBA matrix) *m*/*z* 1143 [(rotaxane+H)$^+$]. Anal. Calcd for $C_{72}H_{66}N_6O_8$: C 75.6, H 5.8, N 7.4. Found: C 75.5, H 5.9, N 7.3.

X-ray Crystallographic Structure Determinations. 6: $C_{66}H_{65}N_6O_{10}$-Cl_3 M = 1208.59, crystal size 0.25 × 0.10 × 0.10 mm^3, monoclinic $P2_1/n$, a = 20.367(2), b = 11.124(1), c = 27.591(2) Å, β = 101.83-(1)°, V = 6118.3(9) Å^3, Z = 4, ρ_{calcd} = 1.312 mg m^{-3}; (graphite monochromated Mo Kα radiation, λ = 0.71073 Å), μ = 0.214 mm^{-1}, T = 150(2) K. 19043 data (8463 unique, R_{int} = 0.3107, 2.00 < θ < 25.00°), were collected on the EPSRC National Service Enraf Nonius Kappa CCD diffractometer with area detector using ϕ and ω scans and were corrected semiempirically for absorption and sample decay (transmission 0.95−0.98). The structure was solved by direct methods and refined by full-matrix least-squares on F^2 values of all data (G. M.Sheldrick, SHELXTL manual, Siemens Analytical *X*-ray Instruments, Madison WI, 1994, version 5) to give $wR = \{\Sigma[w(F_o^2 - F_c^2)^2]/\Sigma[w(F_o^2)^2]\}^{1/2} = 0.132$, conventional R = 0.054 for F values of 1338 reflections with $F_o^2 > 2\sigma(F_o^2)$, S = 0.465 for 768 parameters. Residual electron density extremes were 0.247 and −0.210 Å^{-3}. All non-hydrogen atoms were refined anisotropically. Hydrogen atoms were constrained to chemically reasonable positions.

7: $C_{70}H_{72}Cl_6N_6O_{10}$, M = 1370.09, crystal size 0.30 × 0.30 × 0.10 mm^3, monoclinic $P2_1$, a = 10.964(3), b = 32.032(7), c = 11.285(7) Å, β = 117.72(4), V = 3508(3) Å^3, Z = 2, ρ_{calcd} = 1.297 mg m^{-3}; Cu Kα radiation (λ = 1.5418 Å), μ = 2.729 mm^{-1}, T = 293(2)K. 5649 data (5342 unique, R_{int} = 0.105, 2.76 < θ < 60.12°), were collected on a Siemens SMART CCD diffractometer using narrow frames (0.3° in ω) and were corrected semiempirically for absorption and incident beam decay (transmission 0.62−1.00). The structure was solved by direct methods and refined by full-matrix least-squares on F^2 values of all data (Bruker SMART and Bruker SHELXTL) to give $wR = \{\Sigma[w(F_o^2 - F_c^2)^2]/\Sigma[w(F_o^2)^2]\}^{1/2} = 0.087$, conventional R = 0.058 for F values of 1575 reflections with $F_o^2 > 2\sigma(F_o^2)$, S = 3.28 for 449 parameters. Residual electron density extremes were 0.25 and −0.24 Å^{-3}. Amide hydrogen atoms were refined isotropically subject to a distance constraint N−H = 0.98 Å, with the remainder constrained. Due to the low number of observed data, anisotropic displacement parameters were used only for oxygen and nitrogen atoms with all remainder atoms isotropic.

Experimental details for **8** and **9** were the same as for **7** except for the following. **8**: $C_{67}H_{68}N_6O_{10}S$, M = 1149.33, crystal size 0.002 × 0.080 × 0.100 mm^3, triclinic P1, a = 10.839(10), b = 11.151(10), c = 14.639(2) Å, α = 69.56, β = 83.67, γ = 62.14°, V = 1462.66(3) Å^3, Z = 1, ρ_{calcd} = 1.305 mg m^{-3}; synchrotron radiation (CCLRC Daresbury Laboratory Station 9.8, silicon monochromator, λ = 0.6875 Å), μ = 0.122 mm^{-1}, T = 160(2) K. 9754 data (8170 unique, R_{int}=0.0299, 1.44 < θ < 28.68°), were collected on a Siemens SMART CCD diffractometer using narrow frames (0.3° in ω), and were corrected semiempirically for absorption and incident beam decay (transmission 0.32−1.00). The structure was solved and refined as described above for **7** to give $wR = \{\Sigma[w(F_o^2 - F_c^2)^2]/\Sigma[w(F_o^2)^2]\}^{1/2} = 0.1651$, conventional R = 0.0589 for F values of 7528 reflections with $F_o^2 > 2\sigma(F_o^2)$, S = 1.082 for 799 parameters. Residual electron density extremes were 0.444 and −0.341 Å^{-3}. Amide hydrogen atoms were refined isotropically subject to a distance constraint N−H = 0.98 Å, with the remainder constrained; anisotropic displacement parameters were used for all non-hydrogen atoms. **9**: $C_{73}H_{70}Cl_6N_6O_{10}$, M = 1404.05, crystal size 0.004 × 0.030 × 0.070 mm^3, monoclinic $P2_1$, a=10.993, b = 31.217, c = 11.255(10) Å, β = 118.71, V = 3387.62(3) Å^3, Z = 2, ρ_{calcd} = 1.376 mgmg m^{-3}; synchrotron radiation (CCLRC Daresbury Laboratory Station 9.8, silicon monochromator, λ = 0.68750 Å), μ = 0.318 mm^{-1}, T = 160(2) K. 22328 data (14814 unique, R_{int} = 0.0306, 1.26 < θ < 28.56°) were collected on a Siemens SMART CCD diffractometer using narrow frames (0.3° in ω), and were corrected semiempirically for absorption and incident beam decay (transmission 0.38−1.00). The structure was solved and refined as described above for **7** to give $wR = \{\Sigma[w(F_o^2 - F_c^2)^2]/\Sigma[w(F_o^2)^2]\}^{1/2} = 0.1843$, conventional R = 0.0641 for F values of 10279 reflections with $F_o^2 > 2\sigma(F_o^2)$, S = 0.972 for 897 parameters. Residual electron density extremes were 0.561 and −0.521 Å^{-3}. Amide hydrogen atoms were refined isotropically subject to a distance constraint N−H = 0.98 Å, with the remainder constrained; anisotropic displacement parameters were used for all non-hydrogen atoms.

Crystallographic data for **6**−**9** (excluding structure factors) have been deposited with the Cambridge Crystallographic Data Centre as supplementary publication numbers CCDC-147201 (**6**), CCDC-141368 (**7**), CCDC-141369 (**8**), and CCDC-141370 (**9**).[21]21

UV−Vis and CD Spectroscopy. The electronic absorption spectra were recorded on a Hewlett-Packard 8453 diode array spectrometer at 0.1 mM substrate concentrations using commercially available spectrograde solvents. Circular dichroism measurements were recorded in the range 230−320 nm on a JASCO J-720WI-L spectropolarimeter at 0.1 mM substrate concentrations with a path length of 0.1 cm. The path length allowed the reproducible measurement of CD spectra even in $CHCl_3$ in the range 230−250 nm, despite the strong absorbance of the solvent at these wavelengths. As a control, identical CD measurements were also obtained using a JASCO J630 spectopolarimeter.

Computational Experimental Details. In unoriented samples, in general, and in solution, in particular, the circular dichroism response of a system is proportional to the product of the electronic transition dipole moment, M, and the magnetic transition moment, $\mathcal{M}$.[19] If we label the ground state as 0 and the final state as f, the product $M_i(0f)$-$\mathcal{M}_i(0f)$, with $i = x, y,$ or z, can be nonzero for molecules that belong to point groups in which rotations and translations transform as the same irreducible representation. Following previous work,[9] the spectra were simulated using the semiempirical procedure INDO/S (intermediate neglect of differential overlap/spectroscopic parametrization).[10] The configuration interaction was limited to single excited configurations in the molecular orbital space given by the sum of the π and n orbitals. As a consequence of the large line broadening present in the circular dichroism spectra, to compare experiment and theory it was necessary to convolute the calculated stick spectrum (electronic energies and intensities) with a line shape. Since the experimental data were obtained in solution, the line shape should be described by a Gaussian function.

(19) (a) Rosenfeld, R. Z. *Physik* **1928**, *52*, 161. (b) Michl, J.; Thulstrup, E. W. *Spectroscopy with Polarized Light*; VCH: New York, 1986.

Each line calculated quantum chemically was then broadened by multiplying it by a function $G(\nu) = (e^{-(\nu-\nu_o)^2/a^2}/a\pi^{0.5})$ where ν is the excitation wavenumber, in cm^{-1}, ν_o is the wavenumber of the electronic state, in cm^{-1}, and "*a*" the broadening constant, 3000 cm^{-1}.

The rotaxane structures **6**−**9** were optimized using the MM3[11] model implemented in the TINKER[12] program starting from the geometries provided by *X*-ray crystallography.

To investigate the asymmetric nature of the ICD response, chirality was treated as a continuous geometric quantity that can vary between 0 and 100. This approach follows the model known as the continuous chirality measure (CCM), developed by Avnir and collaborators.[16] In dipeptide rotaxanes, chirality arises from the deviation from a symmetry plane. In this scheme, the plane is not determined a priori and must be found numerically by optimization techniques.[20] The chirality value, *S*, is then calculated as

$$S = \frac{100}{D^2}\sum_i (p_i - \hat{p}_i)^2 \qquad (1)$$

where *D* is a normalization factor given by the distance between the geometrical center of the molecule and the most distant atom, p_i are the atomic coordinates, and $\hat{p}_i$ are the coordinates of the atoms of the nearest structure that contains a symmetry plane. $S = 0$ coincides with ideal symmetry (in this case achirality); $S = 100$ collapses the system to a single point.

Two features of the simulations should be commented upon: The first is the energy location that is over estimated by a few thousand cm^{-1}; the second is the relative ordering of the experimental CD intensities—Gly-L-Ala (**6**) < Gly-L-Phe (**9**) < Gly-L-Met (**8**) < Gly-L-Leu (**7**)—for the main band around 240−250 nm that was not well reproduced by the simulations. This band is due to transitions to electronic states that are a combination of the L_a benzenic states of the two isophthaloyl groups with the L_b benzenic states of the *p*-xylylene fragments and the diphenylmethine stoppers. In previous work on the [2]catenane, i.e., the interlocked dimer of the macrocycle, similar semiempirical calculations yielded 5.6 eV (221 nm) for the energy of the L_a states.[8] The present result of ∼210 nm is consistent with those calculations. Because of the eight phenyl groups present in the molecules, the level of degeneration of the spectroscopic states is high and the differences can be ascribed to a not perfectly balanced description of the interactions between the levels. This did not affect the qualitative use of the simulations in uncovering the actual origin of the CD signal in peptide rotaxanes.

Acknowledgment. This work was supported by the TMR initiative of the European Union through contracts FMRX-CT96-0059 and FMRX-CT97-0097 and a British Council UK-Japan Cooperative Research Travel award. F.Z. acknowledges partial support from the MURST project "Dispositivi Supramolecolari". D.A.L. is an EPSRC Advanced Research Fellow (AF/982324).

Supporting Information Available: Tables of crystal data, structure solution and refinement, atomic coordinates, bond lengths and angles, and anisotropic thermal parameters for the X-ray crystal structures of **6**−**9**. This material is available free of charge via the Internet at http://pubs.acs.org.

JA015995F

(20) Press, W. H.; Teukolsky, S. A.; Vetterling, W. T.; Flannery, B. P. *Numerical Recipes, The Art of Scientific Computing*, 2nd ed.; Cambridge University Press: Cambridge, 1992.

(21) Copies of the data can be obtained free of charge on application to The Director, CCDC, 12 Union Road, Cambridge CB2 1EZ, U.K. (Fax: international code + (1223)336−033. E-mail: teched@chemcrys.cam.ac.uk.)